

## An Experimental Measurement on Transient Thermal Response in a PI-Controlled VAV System

Seo Young Kim<sup>†</sup>, Jeong Woo Moon, Won Nyun Kim

*Thermal/Flow Control Center, Korea Institute of Science and Technology P.O.Box 131, Seoul 130-650, Korea*

**Key words:** VAV system, Stratified thermal model, Homogeneous lumped thermal model, PI control, Thermal response

**ABSTRACT:** The present study performs an experimental measurement on transient thermal response of an air-conditioned space by a variable air volume (VAV) system with a PI (proportional-integral) control logic. A thermal chamber with a PI controlled VAV unit is constructed to verify the previously suggested stratified multi-zone model. The effects of thermal parameters and control parameters such as supply air temperature and PI control factor are investigated by implementing the thermal chamber test. The experimental results obtained show that transient behavior of the air-conditioned space-temperature is in good accordance with the simulation results of the stratified thermal model.

### Nomenclature

$F_o$  : nondimensional parameter, Eq. (3)  
 $F_{o2}$  : nondimensional parameter, Eq. (4)  
 $(MC)_j$  : mass-heat capacity at the  $j$ -th zone [J/°C]  
 $min$  : minimum airflow fraction  
 $n$  : nondimensional time delay, Eq. (7)  
 $PB$  : proportional band of temperature [°C]  
 $PIF$  : PI control parameter  
 $Q$  : internal heat gain [W]  
 $R$  : nondimensional parameter, Eq. (5)  
 $t$  : time [sec]  
 $T$  : space temperature [°C]  
 $T_i$  : initial space temperature [°C]  
 $T_o$  : outdoor temperature [°C]  
 $T_r$  : set point temperature [°C]  
 $T_s$  : supply air temperature [°C]

$(UA)_j$  : heat transmittance from the building envelope at the  $j$ -th zone [W/°C]  
 $(UA)_{j,j-1}$  : heat transmittance between the  $j$ -th and the  $(j-1)$ -th zones [W/°C]  
 $(UA)_{j+1,j}$  : heat transmittance between the  $(j+1)$ -th and the  $j$ -th zones [W/°C]  
 $V_{max}$  : volume flow rate of supply air [m<sup>3</sup>/sec]  
 $x$  : supply airflow rate

### Greek symbols

$\rho c$  : heat capacity of supply air [J/m<sup>3</sup>°C]  
 $\theta$  : non-dimensional temperature, Eq. (2)

### Superscripts

$i$  : time index

### Subscripts

$j$  : zone index  
 $t - td$  : time delay prior to the current time

<sup>†</sup> Corresponding author

Tel.: +82-2-958-5683; fax: +82-2-958-5689

E-mail address: seoykim@kist.re.kr

### 1. Introduction

The main issues in the design and operation of air-conditioning systems are the indoor air quality for human comfort as well as high efficiency for energy savings. For this reason, recently, the variable air volume (VAV) system is widely being used as an air-conditioning system in commercial buildings. The VAV system regulates the volume of supply air to compensate for varying load in a space. Advantages of the VAV system are low initial cost, low operating cost and rapid response to varying loads. In spite of many advantages, however, the VAV system may not provide a comfortable environment until the system is properly operated.

To achieve the efficient operation of a VAV system, it is essential to establish an appropriate VAV system model for the optimal control strategy. Kim et al.<sup>(1)</sup> showed the relationship between the space-averaged temperature and the associated thermal parameters in an air-conditioned space. Lu et al.<sup>(2)</sup> and Zaheer-Uddin<sup>(3)</sup> dealt with air distribution in multi-zone rooms. Zhang and Nelson<sup>(4)</sup> suggested a simple homogeneous lumped thermal model to numerically simulate thermal response of an air-conditioned space by a supply airflow control. The thermal characteristics of an air-conditioned space were expressed by the time variation of a representative space temperature. In an attempt to provide the information on local temperatures of the space, recently, Moon et al.<sup>(5)</sup> suggested a stratified thermal model (multi-zone model) for an air-conditioned space.

In the present study, experiments have been performed to investigate thermal response of a PI-controlled VAV system for a thermal chamber. Time-dependent air temperatures are measured at four elevations of the air-conditioned thermal chamber. The measured thermal response is compared with the analytical predictions based on the stratified thermal model.<sup>(5)</sup>

### 2. Modeling of air-conditioned space

Moon et al.<sup>(5)</sup> suggested a stratified thermal model to linearize transient thermal behavior of an air-conditioned space as shown in Fig. 1. Temperatures at the respective zones are assumed to be  $T_j < T_{j+1}$  for the cooling of the space. Assume that  $(MC)_j$  and  $(UA)_j$  are constants, and  $(UA)_{j,j-1}$  equals to  $(UA)_{j+1,j}$ . Then, the nondimensional equation of the stratified thermal model is:

$$\theta_j^i - \theta_j^{i-1} = \frac{Fo}{n} [(\theta_e - \theta_j^{i-1}) - xR(\theta_j^{i-1} - \theta_{j-1}^{i-1})] + \frac{Fo_2}{n} (\theta_{j+1}^{i-1} - 2\theta_j^{i-1} + \theta_{j-1}^{i-1}) \quad (1)$$

where,

$$\theta_j = \frac{(T_j - T_s)}{PB} \quad (2)$$

$$Fo = \frac{(UA)_j}{(MC)_j} td \quad (3)$$

$$Fo_2 = \frac{(UA)_{j,j+1}}{(MC)_j} td \quad (4)$$

$$R = \frac{\rho c V_{max}}{(UA)_j} \quad (5)$$

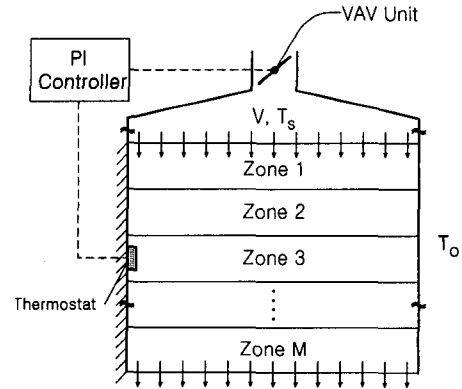


Fig. 1 Schematic of an air-conditioned space.

$$x = (1 - min) \left[ \theta^{1-n} + PIF \Delta T \sum_{k=n}^1 \theta^{k-n} \right] \quad (6)$$

$$min \leq x \leq 1$$

$$n = \frac{td}{\Delta t} \quad (7)$$

Here,  $t$  is the time step for the numerical calculation and  $PIF$  in Eq. (6) denotes the PI control factor. The model prediction used in comparing to the experimental data was carried out based on Eqs. (1)~(7).

### 3. Experimental setup and test procedure

In the present study, a supply air controller was constructed based on the PI control logic in Eq. (6) to carry out an air-conditioning test in a thermal chamber. Fig. 2 shows a schematic diagram of a thermal chamber for the supply airflow control test. The experimental facility consisted of a thermal chamber, an air handling unit and a VAV unit. A thermal chamber of  $3\text{ m} \times 1.7\text{ m} \times 2.75\text{ m}$  was modeled on an office room. To provide a cooling load, an electrical heater was installed in the thermal chamber. The thermal chamber was divided into four zones according to the elevation for temperature measurement as shown in Fig. 3. Sixty T-type thermocouples, i.e., fifteen thermocouples at each zone, were used to measure air temperature distribution in the thermal chamber.

A 3-RT air-handling unit (AHU) was constructed to supply a cooling air to the thermal

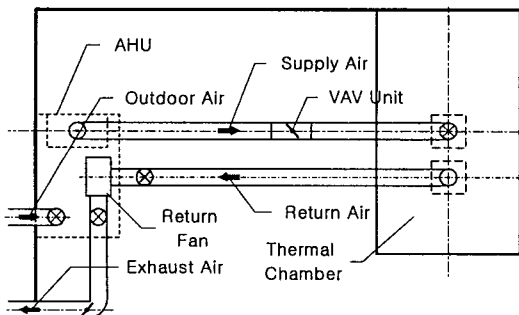


Fig. 2 Schematic of experimental setup.

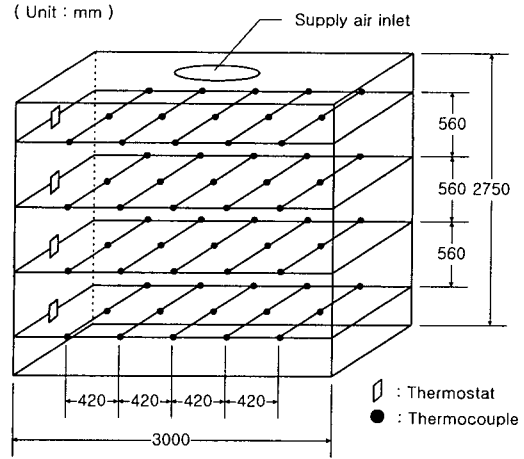


Fig. 3 Air temperature measuring locations in the thermal chamber.

chamber. The maximum flow rate and the static pressure head of the blower inside the AHU were 40 CMM and 40 mmAq, respectively. The AHU supplied cooling air to the thermal chamber through a circular duct with a diameter of 250 mm. A damper type VAV unit with a maximum static head loss of 20 mmAq was used in the present experiment.

The VAV unit managed a cooling load in the thermal chamber by supplying a cool air from AHU to the chamber. The supply air was induced from a diffuser located at the ceiling of the chamber. Return air from the chamber was exhausted in part to the outdoor and then

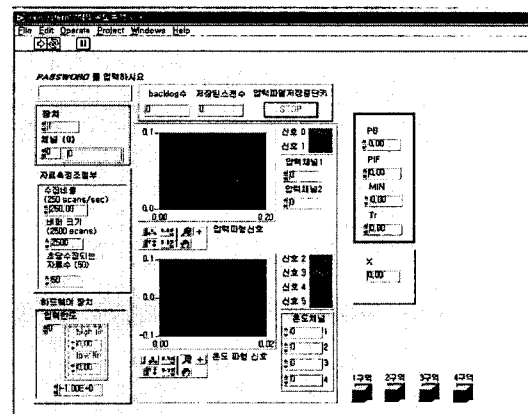


Fig. 4 VAV system control panel.

it was mixed with a fresh outdoor air in the mixing plenum of the AHU.

Representative space temperature for the PI control input was measured by thermostats of Pt 1000 located at the chamber wall. The PI controller shown in Fig.4 adjusted a damper position of the VAV unit according to the discrepancy between the set temperature and the measured space temperature.

Before starting a supply airflow control experiment, the supply air was maintained at 12 °C by operating the AHU. Then, the space set temperature, *PIF* and the maximum supply air volume was set and the space temperature data were acquired. Four cases of maximum supply air volume were tested in the present study. Air temperatures in the air-conditioned space until the steady state were measured and stored in a PC by a data acquisition system.

#### 4. Results and discussion

First, comparison of averaged space air temperatures between the previous model predictions and the present experiment is made at  $T_s=12^\circ\text{C}$ ,  $T_i=20^\circ\text{C}$  and  $T_o=16^\circ\text{C}$ . Internal cool-

ing load is set at  $Q=1000\text{ W}$  and the supply airflow rate is  $V_{\max}=1000\text{ CMH}$ . Total mass-heat capacity of the thermal chamber is  $MC=16647\text{ J}/^\circ\text{C}$ . For the stratified thermal model, mass-heat capacity at each zone is  $(MC)_j=MC/N\text{ J}/^\circ\text{C}$ , where  $N$  is the number of zones. Assume that heat conductance  $(UA)_j=43.23/N\text{ W}/^\circ\text{C}$  by considering mixed convection from the wall and conduction through walls such as glass and wood panel.<sup>(6)</sup> Heat conductance between zones  $(UA)_{j,j+1}$  is also assumed to be  $0.07\text{ W}/^\circ\text{C}$ .

Temporal variation of space air temperature in the thermal chamber is displayed in Fig.5. The prediction by the stratified thermal model of Moon et al.<sup>(5)</sup> shows a general accordance with the present experimental data. However, the simulation result by the homogeneous lumped thermal model shows considerable discrepancy from the initial stage.

Figure 6 shows the temporal variation of space temperatures in the thermal chamber. Temperature difference of 4°C to 6°C can be clearly seen according to the elevation. It is noted that the stratified thermal model generally follows

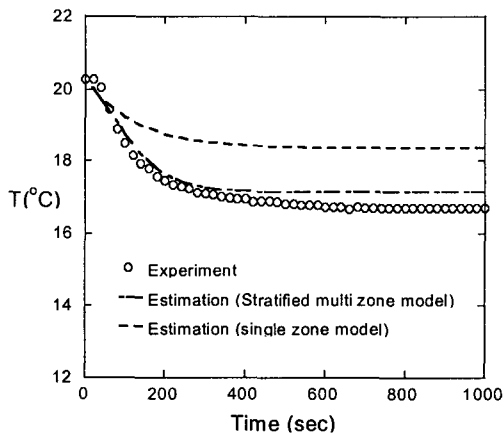


Fig. 5 Transient behavior of mean temperature.  $T_i=20^\circ\text{C}$ ,  $T_o=16^\circ\text{C}$ ,  $Q=1000\text{ W}$ ,  $V_{\max}=1000\text{ CMH}$ ,  $Fo=2.59 \times 10^{-2}$ ,  $Fo_2=4.2 \times 10^{-5}$ , and  $R=7.46$ .

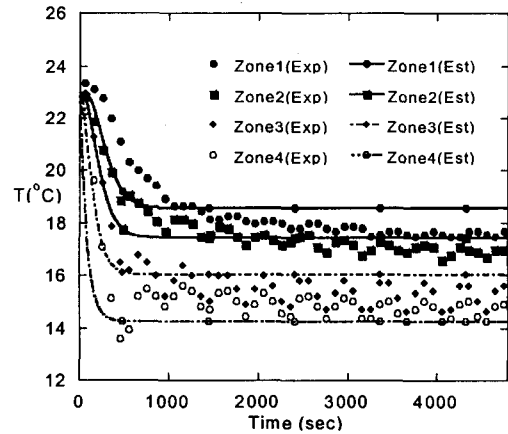


Fig. 6 Transient behavior of space temperature.  $T_s=12^\circ\text{C}$ ,  $T_r=17^\circ\text{C}$ ,  $V_{\max}=500\text{ CMH}$ ,  $Fo=2.59 \times 10^{-2}$ ,  $Fo_2=4.2 \times 10^{-5}$ ,  $R=4.66$ ,  $PB=5^\circ\text{C}$ , and  $PIF=0$ .

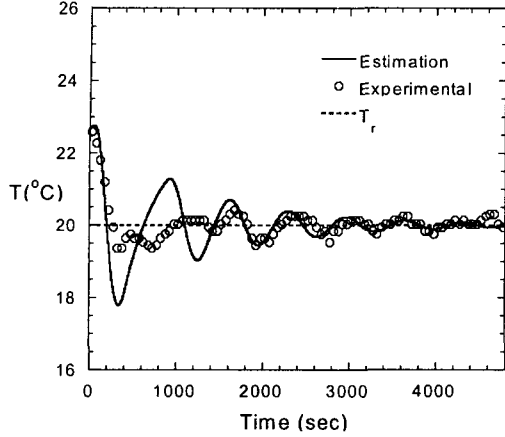


Fig. 7 Transient behavior of third zone temperature.  $T_s=12^\circ\text{C}$ ,  $V_{\max}=600$  CMH,  $Fo=2.59\times 10^{-2}$ ,  $Fo_2=4.2\times 10^{-5}$ ,  $R=4.66$ ,  $PB=5^\circ\text{C}$ , and  $PIF=0.01$ .

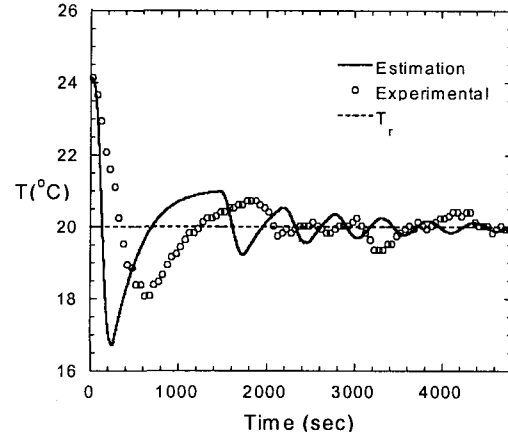


Fig. 8 Transient behavior of third zone temperature.  $T_s=12^\circ\text{C}$ ,  $V_{\max}=1000$  CMH,  $Fo=2.59\times 10^{-2}$ ,  $Fo_2=4.2\times 10^{-5}$ ,  $R=7.46$ ,  $PB=5^\circ\text{C}$ , and  $PIF=0.01$ .

the actual variation of space temperature in the thermal chamber although the experimental data present some fluctuation in space temperatures.

Figure 7 exhibits the temporal variation of space temperature at  $T_s=12^\circ\text{C}$ ,  $V_{\max}=600$  CMH, and  $PIF=0.01$ . The predicted results based on the stratified thermal model are in overall agreement to the experimental data. However, the model prediction shows much larger fluctuation than the experimental data at the early stage. It is attributed that the actual airflow in the thermal chamber is laterally mixed while the one-dimensional model prediction excludes such effects. Consequently, the effect of lateral mixing reduces the amplitude of spatial temperature fluctuation. After achieving a stable flow field, the predicted temperature shows a good agreement to the actual temperature variation.

Temporal variation of space temperature in the thermal chamber for a higher supply airflow rate of  $V_{\max}=1000$  CMH is shown in Fig. 8. Predicted temperature variation at the early stage shows a large discrepancy with the experimental measurement due to the enhanced lateral flow mixing as the airflow rate increases. In general, however, the airflow rate

to a room in modern air-conditioning systems is less than  $V_{\max}=1000$  CMH. Therefore, it is believed that the stratified thermal model provides accuracy enough to predict actual behavior of space temperature.

Figure 9 shows the effect of  $PIF$  on temporal variation of space temperature at  $V_{\max}=800$  CMH. As  $PIF$  increases, thermal response of

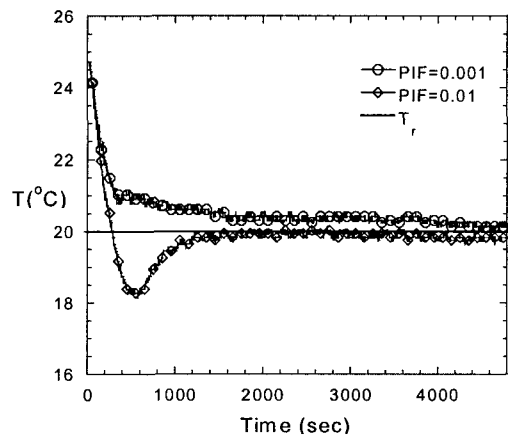


Fig. 9 Effect of  $PIF$  on temporal variation of third zone temperature.  $T_s=12^\circ\text{C}$ ,  $V_{\max}=800$  CMH,  $Fo=2.59\times 10^{-2}$ ,  $Fo_2=4.2\times 10^{-5}$ ,  $R=4.66$ , and  $PB=5^\circ\text{C}$ .

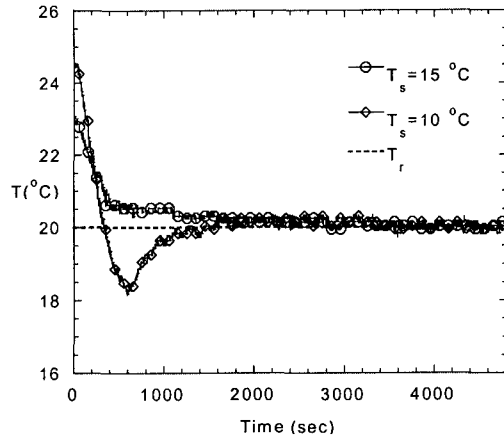


Fig. 10 Effect of  $T_s$  on temporal variation of third zone temperature.  $V_{\max}=600$  CMH,  $F_{O_1}=2.59 \times 10^{-2}$ ,  $F_{O_2}=4.2 \times 10^{-5}$ ,  $R=4.66$ ,  $PB=5^\circ\text{C}$ , and  $PIF=0.001$ .

space becomes unstable. It is attributed to the inappropriate selection of  $PIF$  in the PI controller,<sup>(5)</sup> which results in improper compensation of error between the set temperature and the measured space temperature.

Influence of  $T_s$  on temporal variation of space air temperature is displayed in Fig. 10. As  $T_s$  decreases, the over cooling occurs at the early stage. This is caused by the fact that, for low  $T_s$ , a small change of airflow rate produces a relatively large change of space air temperature and results in the instability of the system. As the proportional band of temperature  $PB$  increases, however, space temperature may vary stably for low  $T_s$ , because of increased mass-heat capacity of the space.

## 5. Conclusion

An experimental study of supply airflow control in a variable air volume (VAV) system has been carried out. Transient thermal response of an air-conditioned space was measured and compared with the prediction results by the stratified thermal model.

The results obtained showed that the stratified thermal model predicted well the transient behavior of space air temperature by a VAV unit up to a moderate flow rate. The homogeneous lumped thermal model showed considerable discrepancy compared to the experimental data. Thermal stratification was also observed at an actual air-conditioned space. It was noted that the location of thermostat was crucial in the supply airflow control of a VAV system. In the supply airflow control of a VAV system, the PI control parameter  $PIF$  and the supply air temperature  $T_s$  influenced strongly on thermal response of the air-conditioned space.

## Acknowledgment

The present work was supported by a grant from the Regional Research Center for Air-Conditioning Technology in Sunmoon University, South Korea.

## References

1. Kim, W.N., Kim, S.Y., Kang, B.H. and Hyun, J.M., 1998, A numerical simulation on room temperature measurement method for VAV system control, Proceedings of the SAREK'99 Summer Annual Conference, pp. 379-383.
2. Lu, W., Howarth, A.T., Adams, N. and Riffat, S.B., 1999, CFD modeling and measurement of aerosol particle distributions in ventilated multi-zone rooms, ASHRAE Transaction, Vol. 106, pp. 116-127.
3. Zaheer-Uddin, M., 1993, Energy start-stop and fluid flow regulated control of multi-zone HVAC systems, Energy, Vol. 18, pp. 289-302.
4. Zhang, Z. and Nelson, R.M., 1992, Parametric analysis of a building space conditioned by a VAV system, ASHRAE Transaction, Vol. 98, pp. 43-48.

5. Moon, J. W., Kim, S. Y., Kim, W. N. and Cho, H. H., 2000, Simulation of supply air control in a VAV system using a stratified lumped thermal model, *Journal of SAREK*, Vol. 12, pp. 632-641.
6. Mills, A. F., 1995, *Basic Heat and Mass Transfer*, 1st ed., Richard D. Irwin, Inc., pp. 274-279.